

## Chapter 2

# Material Development and Process

Recently, there has been a significant increase of interest in fabricating oxide materials that consist of nanosized particles ranging in mean diameter from 1 to 100 nm. The interest in these materials has been stimulated by the fact that, owing to the small size of the building blocks (particles, grain or phase) and the high surface-to-volume ratio, these materials are expected to demonstrate unique mechanical, optical, electronic and magnetic properties. The fabrication of these materials of perfect nanometre-scale crystallites, identically replicated in unlimited quantities in such a state that they can be manipulated and understood as pure macromolecular substances, is an ultimate challenge in modern materials research with outstanding fundamental and potential technological consequences. Interest in magnetic nanoclusters has increased in the past few years by virtue of their novel properties, which have promising broad spectrum applications from biological tagging to recording devices [1–6]. Significantly,  $\gamma\text{-Fe}_2\text{O}_3$  is considered to be the most promising material in this group and is currently finding a variety of applications [7–11]. Therefore, the idea of synthesizing iron oxide particles in their nanocrystalline form for the purpose of superior technological and wider commercial exploitation is gaining a lot of momentum.

Many novel processing techniques have been developed so far to synthesize ultrafine iron oxide powder, e.g. hydrothermal reaction [12], plasma-enhanced chemical vapour deposition [13], sol–gel synthesis [14], spray pyrolysis [15], flame pyrolysis [16] and mechanical activation [17]. However, most of these processes suffer from some serious limitations. First, stringent control over various process parameters is required and secondly, production yield is very low and obviously, not cost effective. In some processes, due to high energy of activation, the resulting powders often exhibit poor particle characteristic represented by a wide particle size distribution and irregular particle morphology, together with a substantial degree of particle aggregation. In addition to the above, most processes require high energy and sophisticated instrumentation. In view of these limitations, the present investigation was primarily designed with an objective to develop a simple and reliable preparation technique, which will involve low temperature treatment, low energy consumption and minimum requirements for sophisticated instrumentation.

One of the most commonly used techniques to produce monodispersed particles (uniform in size and shape) is precipitate from homogeneous solutions [18], which can be employed for the preparation of uniform colloidal particles. However, almost all studies have been confined to aqueous solutions and little attention has been paid to non-aqueous media. It is to be noted that in aqueous route, a small change in the salt concentration or in the pH over critical regions produces particles of different chemical composition and morphology. Moreover, the growth of the particles cannot be restricted in the aqueous medium during precipitation. In contrast to the above, in non-aqueous route, one may proceed by decomposition of organometallic compounds that will eventually yield uniform particles. In recent times, organic fatty acids, e.g. stearic acid, oleic acid, palmitic acid, etc., are used as the precursors for this purpose [18–20]. Considering these aspects, an attempt has been made here to prepare monodispersed and uniform particles of iron oxide from an organic precursor of stearic acid (Fig. 2.1). This will be followed by the evolution kinetics study of  $\gamma$ -Fe<sub>2</sub>O<sub>3</sub> nanoparticles from the organic precursor during heating.

The synthesis of  $\gamma$ -Fe<sub>2</sub>O<sub>3</sub> nanoparticles is based on the decomposition and subsequent reduction of the intermediate/complex of Fe(O)(stearate) obtained by thermolysis of iron(III) nitrate in a non-aqueous stearic acid medium. The synthesis procedure was as follows. A homogeneous solution was prepared by gradual addition of a calculated amount of Fe(NO<sub>3</sub>)<sub>3</sub> · 9H<sub>2</sub>O to a known amount of molten stearic acid. To have controlled synthesis, the molar ratios of stearic acid to hydrated Fe(III) nitrate was taken in an optimized ratio. The homogeneous solutions prepared with the above composition were thermolyzed separately at 125 °C until evolution of brown fumes of NO<sub>2</sub> ceased. At this stage, the solution became viscous. The viscous mass was allowed to cool and solidify in air. The solidified mass so obtained was treated with 80 ml of tetrahydrofuran (THF) from which the precipitates were collected by centrifugation. The precipitated mass was then dried at 70 °C in an air oven for several hours.

The chemical and compositional characteristics of the as-prepared sample were analysed by FTIR spectroscopy analysis. Figure 2.2 represents the FTIR spectrum of the as-prepared powder precipitates. The peaks observed in the spectrum at 692 and 788 cm<sup>-1</sup> can be assigned to the deformation vibration of Fe–OH groups and the band with the peak at 3285 cm<sup>-1</sup> is assigned to the O–H stretching vibration of the above group. O–H bending vibration is reflected in the spectrum by the peaks observed at 1042 and 1108 cm<sup>-1</sup>. The peak observed at 1355 cm<sup>-1</sup> can be assigned to the characteristic—CH<sub>3</sub> bending vibration. Presence of nitro compounds (C–NO<sub>2</sub>) is indicated by the band observed between 1475 and 1702 cm<sup>-1</sup>. The peaks observed at 2835 and 2904 cm<sup>-1</sup> can be assigned to C–H stretching vibration. The above spectroscopic observations suggest that the as-prepared powder sample consist of residual stearic acid, nitro compounds and FeOOH in an intermediate/complex of Fe(O)(stearate).

The surface functionalities of the as-prepared sample have been investigated by XPS characterization. Figure 2.3 presents the C1s and O1s XPS spectra for the sample. This stearic acid coated sample shows a rather complex composition of the C1s peak, where at least four different components are present. Aliphatic carbon

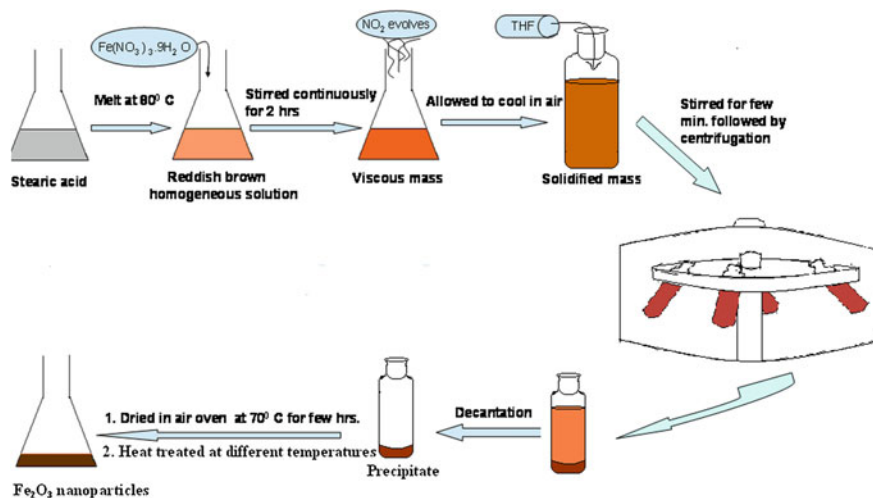


**Fig. 2.1** Schematic diagram of synthesis of iron oxide nanoparticles

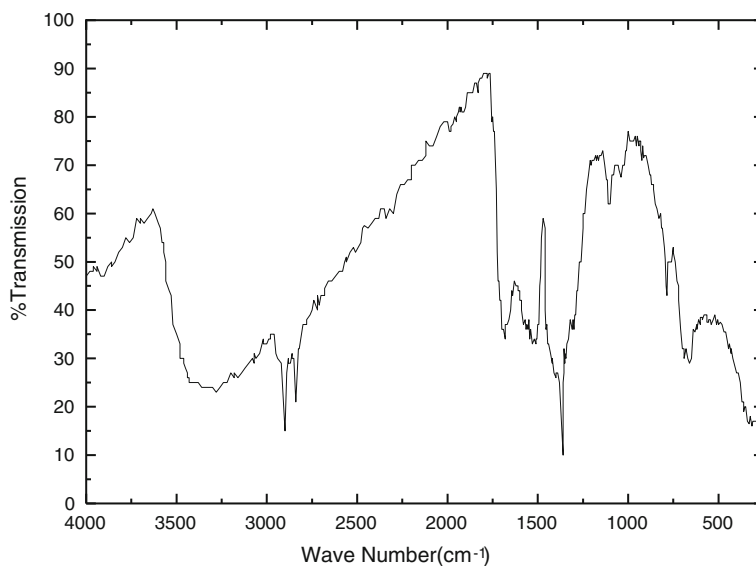
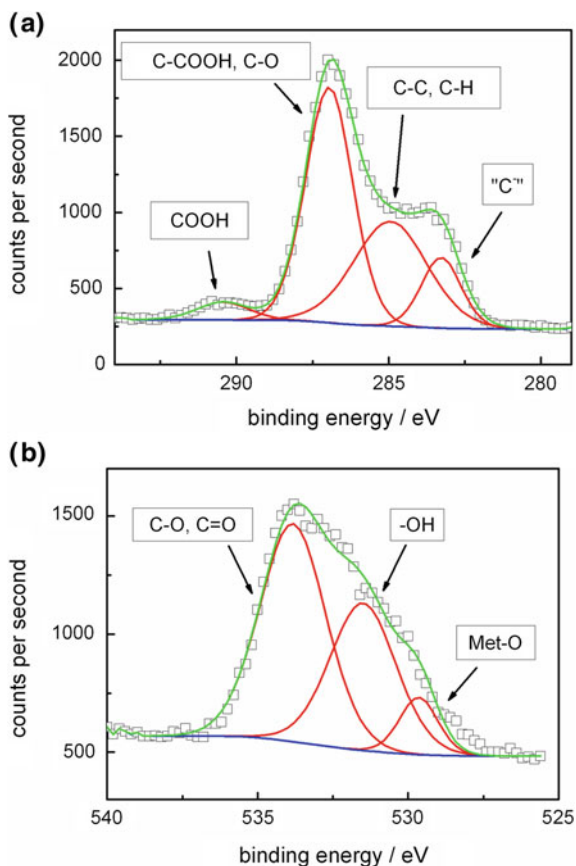


**Fig. 2.2** FTIR spectrum of the as prepared powder precipitates

from stearic acid is present at 285 eV [21]. Two peaks at higher binding energies, 287 and 290.2 eV, are for the carbon atoms in the vicinity of oxygen which indicates to the C atoms of carboxyl group, respectively [22]. In addition, one peak at 283.2 eV can be explained by carbon in contact with an electropositive species which points towards the probability of formation of carbide or something else

**Fig. 2.3** High resolution XP spectra of as prepared sample on Si wafer in **a** C1s and **b** O1s regions



which needs more careful observation [23]. The O1s region also contains several components; three are easily distinguishable; among them the peak at 533.8 eV is due to oxygen bound to carbon [22]. Another peak at 531.5 eV is due to the presence of  $-\text{OH}$  groups which may come from the iron oxyhydroxides ( $\text{FeOOH}$ ) formed during synthesis [24]. The peak at 529.7 eV is due to iron oxide [25]. It is worthwhile to mention here that survey scans show almost no signal of Fe. This means that there is a thick shell ( $>5$  nm) of organic material around the particles.

The XPS investigation into the surface characteristics of the sample with stearic acid as surfactant concludes that the resulting particles have a thick shell ( $>5$  nm) of organic material around the inorganic part, which implies that the stearic acid coating consists of more than one layer. Presence of strongly and weakly bound stearic acid layers over sample surface is evidenced.

Nanosized particles of  $\gamma\text{-Fe}_2\text{O}_3$  were obtained by non-isothermally heating the precipitates from room temperature to 300 °C. The desired temperature of the furnace was controlled by a proportional integral and derivative (PID) controller with an accuracy of  $\pm 1$  °C.

## References

1. Skumryev V, Stoyanov S, Zhang Y et al (2003) *Nature* 423:850
2. Sarikaya M, Tamerler C, Jen A et al (2003) *Nat Mater* 2:577
3. Sun S, Murray CB, Weller D et al (2000) *Science* 287:1989
4. Niemeyer CM (2001) *Angew Chem Int Ed Engl* 40:4128
5. Thompson DA, Best JS (2000) *IBM J Res Dev* 44:311
6. Kodama RH (1999) *J Magn Magn Mater* 200:359
7. Buriak JM (2004) *Nat Mater* 3:847
8. Pankhurst Q, Connolly J, Jones SK et al (2003) *J Phys D Appl Phys* 36:R167
9. Ngo AT, Pileni MP (2001) *J Phys Chem B* 105:53
10. Hyeon T, Lee SS, Park J et al (2001) *J Am Chem Soc* 123:12798
11. Sugimoto M (1999) *J Am Ceram Soc* 82:269
12. Sahu KK, Rath C, Mishra NC, Anadn S, Das RP (1997) *J Coll Interf Sci* 185:402
13. Liu Y, Zhu W, Tan OK, Shen Y (1997) *Mater. Sci. Engg. B* 47:171
14. Sugimoto T, Sakada K (1992) *J Coll Interf Sci* 152:587
15. Morales MP, de Julian C, Gonzales JM, and Serna CJ (1994) *J Mater Res* 9 135
16. Grimm S, Schultz M, Barth S, Miller R (1997) *J Mater Sci* 32:1083
17. Liu X, Ding J, Wang J (1999) *J Mater Sci* 14:3355
18. Matijevic E (1993) *Chem Mater* 5:412
19. Cheng FX, Jia JT, Xu ZG, Zhou B, Liao CS, Yan CH (1999) *J Appl Phys* 86:2727
20. Shafi KVPM, Gedanken A, Prozorov R, Balogh J (1998) *Chem Mater* 10:3445
21. Beamson G, Briggs D (1992) *High resolution XPS of organic polymers: the scienta ESCA 300 database*. Wiley, New York
22. Dilks A (1981) *J. Polym Sci Polym Chem Ed* 19:1319. Standard reference data. <http://www.nist.gov/srd/>
23. Goretzki H, Rosenstiel PV, Mandziej S, Fres. *Anal.Z* (1989) *Chem.* 333:451. Standard reference data. <http://www.nist.gov/srd/>
24. McIntyre NS, Zetaruk DG (1977) *Anal Chem* 49:1521
25. Haber J, Stoch J, Ungier L (1976) *J Electron Spectrosc Relat Phenom* 9:459

Kinetics of Heterogeneous Solid State Processes

Deb, P.

2014, VII, 49 p. 27 illus., Softcover

ISBN: 978-81-322-1755-8